Available online at www.sciencedirect.com

ScienceDirect

Procedia Structural Integrity 33 (2021) 887–895

Structural Integrity Procedia

www.elsevier.com/locate/procedia

IGF26 - 26th International Conference on Fracture and Structural Integrity

Preliminary in-situ study of FIB-assisted method for aluminium solid-state welding at the microscale

Ambra Celotto[a]*, Øystein Grong[a,b], Randi Holmestad[c], Jørgen A. Sørhaug[c], Jan Torgersen[a], Per Erik Vullum[c], Filippo Berto[a]

[a]*Department of Mechanical and Industrial Engineering, Norwegian University of Science and Technology, Richard Birkelands vei 2B, 7491 Trondheim, Norway*

[b]*HyBond AS, NAPIC, Richard Birkelands vei 2B, 7491 Trondheim, Norway*

[c]*Department of Physics, , Norwegian University of Science and Technology, Høgskoleringen 5, 7491 Trondheim, Norway*

Abstract

In situ studies allow real time monitoring and deep comprehension of phenomena. This approach has been applied to the current research for the development of a novel solid-state welding technique at the microscale. The downscaling of the process has been inspired by Cold Pressure Welding (CPW) working principles and it has been carried out by a tailored setup of a high-resolution Focused Ion Beam – Scanning Electron Microscope (FIB-SEM).

This work is primarily aimed at showing how FIB functionalities can be expanded and discussing the challenges that may be encountered by doing that. Therefore, a preliminary FIB-assisted methodology for cold bonding of AA1070 and AA6082 aluminium alloys at the microscale is presented. In situ cross-sectioning of the weld and proper scanning-electron imaging have revealed that, under certain pressure conditions, oxide-free aluminium interfaces are able to be joined at room temperature even at the microscale. Experimental technique improvement and testing of the obtained joints are the next steps needed in this research.

Keywords: microjoining; solid-state welding; cold pressure welding; Focused Ion Beam; electron microscopy; aluminium alloys.

* Corresponding author. Tel.: +39-347-060-3897.
E-mail address: ambra.celotto@ntnu.no

10.1016/j.prostr.2021.10.099

1. Introduction

The ever-increasing miniaturization of a wide variety of devices have boosted innovation, in the late decades, in the field of micro and nanofabrication. Spacing from sensors to computation and control systems, this phenomenon has created opportunities for the manufacturing of electronic, mechanical and optical components (Guo (2008)). In this context, the joining step covers a crucial role in the fabrication process, being able to either strengthen or weaken the final product.

Examples of small-scale welding are reported by Wagle and Baker (2015) employing techniques as ion beam deposition, thermal heating, laser heating, ultrasonic irradiating, high-energy electron beam bombardment and joule heating. Successful joints between metals, semiconductors or ceramic nanowires have been realized through local heating applied by employing voltage or current, heating of the sample stage, laser or electron beam focused onto the coupling sections (Rodriguez-Manzo et al. (2009); Misra and Daraio (2009)). However, these techniques share some inherent limitations concerning the application of local heating. Heating indeed represents a difficult parameter to control at such small scale and, by inducing melting, increases the risk of microstructural and morphological changings in the underlying substructures, thus leading to a sensible modification of the properties of the original building blocks (Wagle and Baker (2015); Lu et al. (2010); Misra and Daraio (2009); Rodriguez-Manzo et al. (2009)). The onset of weaking heat-affected zones and the formation of heterometallic compounds are typical factors that can degrade the joint efficiency. Added to that, expensive instruments, rigorous procedures and tedious operations severely affects their widespread application and reproducibility (Wagle and Baker (2015)). Thus, the need for examples of welding techniques that do not involve the employment of heating are strongly required in the field. In this regard, a major achievement has been shown by Lu et al. (2010) concerning the cold-welding of gold nanowires (from 3 to 10 nm in diameter). It has been proved that mechanical contact alone, at that scale, is enough to obtain a joint that presents nearly the same mechanical and electrical properties of the rest of the nanowire and that preserves a homogenous crystal orientation along that.

An effective procedure to cold bond at the microscale two aluminium alloys is what is being pursued in this research. Aluminium alloys play a strategic role in the manufacturing market of micro and nanocomponents thanks to its considerable weight-specific strength, its low-cost, its high recyclability and above all its good electrical conductivity. For this purpose, a Focused Ion Beam microscope is employed for performing in-situ studies on the suggested technique. To the candidate’s knowledge, this has not yet been reported before for low temperature welding processes at the same scale.

Moreover, the method proposed at the microscale is expected to give some deeper insights on the bonding mechanisms occurring also at the macroscale for established cold-welding processes. In particular, the innovative hybrid metal extrusion & bonding (HYB) process, developed and patented in the recent years by people in the research group, stands out for its noticeable flexibility in terms of geometry and number of different materials that can be joined, its low exercise temperature and its resulting high-performances joints (Grong, Sandnes, and Berto (2019a); Grong, Sandnes, and Berto (2019b); Sandnes et al. (2021); Sandnes et al. (2018); Grong (2006); Aakenes, Grong, and Austigard (2014)). Although HYB apparatus is quite difficult to be downscaled inside a FIB, it will serve both as a starting point and a target for the designing of the microscale experiments.

The in-situ approach was chosen for the better understanding it generally allows of phenomena thanks to several opportunities that offers: real time process monitoring, localized investigations and testing and the possibility of 3D reconstruction. In this case, some challenges raised too, such as the downscaling of the welding process and the further optimization of the joints’ properties. Hence, this preliminary study is aimed at suggesting an experimental method for a FIB-assisted cold welding of aluminium at the microscale and discussing its advantages and side effects. A way to expand FIB’s potentiality is also presented through a microscope tailoring procedure.

The experiments will be here presented in a chronological order, starting from their designing in relation to the instruments and the examples available at the state of the art, to their development and modification in progress.

2. Design of experiments

A high-resolution dual-beam platform microscope was employed both to carry out and to real-time monitor the joining process and its results. The downscaled welding setup was inspired by the working principles of Cold

Pressure Welding and the geometry of the HYB process. An AA6082 aluminium alloy thin plate was employed as Base Metal (BM), while an AA1070 wire served as Filler Metal (FM).

2.1. Focused Ion Beam (FIB) microscopy

In this section, a brief overview on the architecture and the possible applications of dual-beam microscope is given. This is based on previous broader works such as Volkert C. A. (2007); Munroe (2009); Sugiyama and Sigesato (2004); Sezen (2016).

With the term FIB is commonly intended a FIB-SEM, namely a dual-beam system that consists of a Scanning Electron Microscope equipped also with an Focused Ion Beam source, typically Ga^+, and other tools dedicated for nano-machining and nano-prototyping procedures. This kind of instrument combines the high-resolution low-damage imaging capabilities of scanned electrons with FIB's selective and precise milling. Indeed, an accurate control of the ion beam parameters - such as position, current and dwell time - allows customized nanostructures to be locally fabricated or reshaped, by following predefined scan patterns. The effect of energetic ions focused on a sample consists in sputtering of material particles that ends up in an eroded surface. Fig.1 shows a schematic representation of the main tools composing a FIB instrument. Depending on the manufacturer and the model, the ion column is tilted with respect to the electron column of an angle that typically varies vary from 52 and 55°. This setup gives access to a double imaging perspective on the working area, letting the user check in real-time the fabrication process.

A major role is covered in this work by the micromanipulator with which the FIB is equipped. This consists of an interchangeable tungsten (W) needle that can be moved and controlled through a dedicated software. It is primarily meant for *lift-out* operations and transfer of small material pieces inside the microscope chamber. In order to make the needle grab the particles to be moved, a layer of organic material is commonly deposited firmly both on the sample and on the needle tip surfaces to glue them together. For doing this, a precursor-based Gas Injection System (GIS) is typically integrated in the instrument for Chemical Vapour Deposition (CVD). A variety of chemical species is available for being added to the system, but platinum and carbon are the most frequently employed for deposition of gluing or protection layers on the sample surface. As in a regular SEM, different types of detectors may be integrated, the ones for chemical analysis included.

Currently, the main application of FIBs is an advanced technique for TEM sample preparation, but they are also employed for computer chip repair, circuit modification and 3D tomography by means of serial slicing.

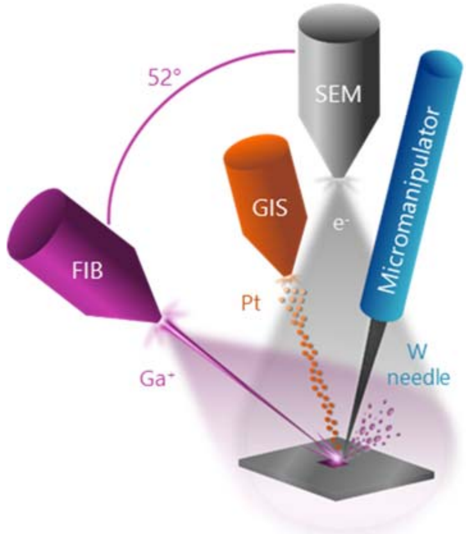

Fig. 1. Schematic representation of a Focused Ion Beam- Scanning Electron Microscope operating on a sample and the tools with which it is typically equipped: an electron and ion columns for high resolution imaging, a Focused Ion Beam (FIB) for material milling, a Gas Injection System (GIS) for Chemical Vapour Deposition and a micromanipulator for transfer of material pieces.

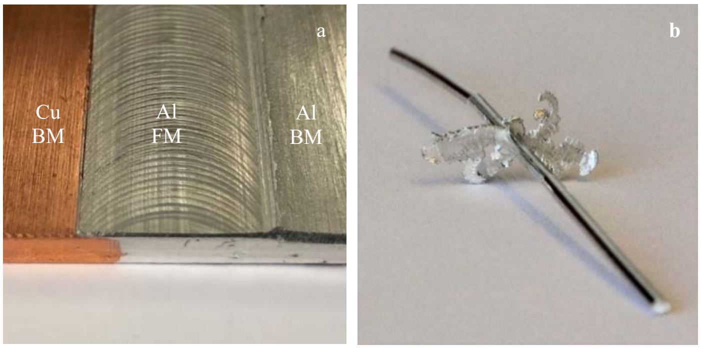

Fig. 2. Metallic joints fabricated by means solid-state welding techniques that are considered as macroscale reference in this work: (a) Copper-aluminium joint obtained by Hybrid metal extrusion & Bonding (HYB); (b) Aluminium-aluminium Cold Pressure Welded (CPW) joint with its flash.

2.2. FIB-assisted welding procedure

The welding experiments of this research are aimed at reproducing HYB bonding conditions as closely as possible at the microscale. To make the downscaled process feasible inside the FIB chamber some simplifications were required and are here discussed.

HYB process is a very versatile welding technique (Grong, Sandnes, and Berto (2019b); Sandnes et al. (2018)) based on the continuous extrusion of a metallic filler wire for obtaining multi-material butt-joints (Fig.2a). A rotating pin drags the filler wire and forces it to pass in a smaller die to be then squeezed outside. The extruded wire is continuously fed inside an existing groove between the base materials to be welded. While doing that, the filler metal is stirred by the pin vigorously together with the base material interfaces, while being mixed and highly deformed, achieving at the end a strong bond at the room temperature.

For the microscale experiment instead, diversely from the reference HYB process, it has been chosen to couple only one Base Metal (BM) with a Filler Metal (FM). This is expected to be enough for representing one side of the regular HYB-joint. Two aluminium alloys were employed to facilitate the bonding mechanism at room temperature: an AA1070 BM and an AA6082 FM. Indeed, the bonding mechanism between similar metals does not imply atoms diffusion, but it is achieved by sharing of valence electrons, which in the case of aluminium are in number of three. Full metallic bonding is expected to be reached at the interface of the two.

Because of some manufacturing and geometrical constraints that impede HYB process from being directly downscaled, the extrusion setup had to be replaced by a simpler FM feeding technique. Therefore, the inspiration was taken from Cold Pressure Welding (CPW), a simple and very efficient solid-state joining technique that has been described in detail by Bay (2018) and Iordachescu et al. (2009). By means of this method, it is possible to cold weld wires, bars, or plates only by bringing them into close contact under a certain pressure (Fig.2b). The process is carried out with special clamps in which the two workpieces are secured with their free ends protruding externally. By the application of a load, the free ends are pressed one against the other resulting in severe axial plastic deformation; the original external ends are brought into the flash while the inner original virgin surfaces create a strong bond (Fig.2). This can be performed up to six times on the same workpieces and, in the case of aluminium-aluminium joints, the weld area typically presents a higher mechanical strength and microhardness than the BMs, without compromising their electrical conductivity.

Being both CPW and HYB processes solid-state welding processes, in which plastic deformation plays the biggest role in the bond formation, CPW seemed to be an ideal candidate to be mimed and downscaled in the FIB thanks to its higher geometrical simplicity compared to the target HYB. Therefore, the FIB apparatus needs to be tailored for this purpose.

Thus, the here suggested procedure for cold bonding aluminium at the microscale is mainly based on CPW principles and the use of the FIB's micromanipulator. Basically, the method exploits the micromanipulator as an actuator that provides the required force to deform and weld the materials (CPW-like pushing). At the same time, its moving capabilities are used for continuously feeding the FM to be joined along a predefined path on the BM

(CPW-like feeding, HYB-like FM deposition). To do that, the tip of the tungsten needle must be replaced with an aluminium FM tip by means of the *lift-out* FIB-assisted procedure better explained in Section 3.1. The result is a hybrid needle, made of tungsten and an aluminium tip. The FM tip is expected to be deposited and then bond to the BM sample under the pressure applied by the micromanipulator.

3. Materials and methods

As mentioned above, the experimental apparatus consists of an Al-tip needle pushed against an Al base plate by means of a FIB microscope. The pushing procedure is meant to be operated by the micromanipulator with which the FIB is equipped, the Omniprobe® manipulator in this case. This is provided with a very sharp tungsten needle, which can be interchanged. The tip of this needle was replaced with an Al-tip (FM) by means of the procedure described below. The instrument used is a FEI Helios NanoLab DualBeam FIB, which has Omniprobe® dedicated software that allows the manipulator to be moved along its own axis. The BM sample was a raw AA1070 1.5 mm thick plate, whereas the FM tip was extracted from a AA6082 wire, 1.4 mm in diameter, that has been mechanically polished into a 6° tapered wedge.

3.1. FIB-assisted needle tip replacement

The steps followed for the tungsten needle tip replacement with the aluminium one are similar to the established procedures for TEM sample preparation that can be found for example in Mayer et al. (2007).

A new Omniprobe® tungsten needle is loaded on the FIB stage, as a regular sample, together with the polished FM wedge (Fig.3a). By ion milling, an approximately 35 μm long FM tip is cut out from the AA6082 wedge and a thin bridge is left for holding it (Fig.3c). The operating Omniprobe® needle mounted on the micromanipulator is then made approaching and gently touching the pre-shaped FM tip. The needle is glued to the tip by a 1 μm thick layer of deposited platinum, by the GIS. The tip is now held both by the micromanipulator, through the platinum pad, and by the bulk wedge, by the bridge. The bridge is then milled away, leaving the tip hung only to the Omniprobe® manipulator, so that it can be lifted out from the bulk wedge.

On another side of the stage, there is the tungsten needle and this is oriented in the same direction of lifted FM tip. By a cleaning cross-section ion-milling pattern, the tungsten needle tip is removed, obtaining a virgin flat surface perpendicular to the needle axis (Fig.3b). The FM tip, that is hung to the Omniprobe® manipulator, is transferred close to the flat face of the truncated tungsten needle and, once the two flat surfaces matched each other at their highest point, platinum pads are deposited in all the coupling zone that is accessible from the ion beam perspective. Once the tip is firmly anchored to the tungsten truncated part, the Omniprobe® manipulator can be detached from the tip by ion milling of the platinum bond (Fig.3d).

The result has to be considered as a “raw hybrid needle”: due to the original shape of the FM wedge, the FM tip must be now shaped in a needle-like way and a robust platinum “ring” needs to be deposited all around the coupled interface to make the tip integral with the needle. For doing so, this “raw hybrid needle” is mounted in the Omniprobe® shaft and inserted in the FIB. This allows the needle to be rotated on its own axis and, by exposing different sides of the tip to the ion beam, the tip can be smoothened and welded, by ion milling and chemical vapour deposition respectively. Once the tip has reached a satisfying conical and sharp shape, and a reliable platinum ring has been created, the hybrid needle is ready to be employed both as actuator and feeder in the microscale welding setup (Fig.3e).

4. Preliminary results and discussion

Being the very first pushing attempt inside a FIB, the welding experiment itself is here recognized as a preliminary result, able to tell whether the setup geometry, the materials involved and the platinum link Al-W can bear efficiently the applied load by reaching plastic deformation and preventing it from premature failing.

The first configuration adopted revealed not be effective, but the resulting situation permitted to proceed the experiment and adapt the setup locally in real-time. The pushing procedure was conducted, and a bonded interface was identified and analyzed.

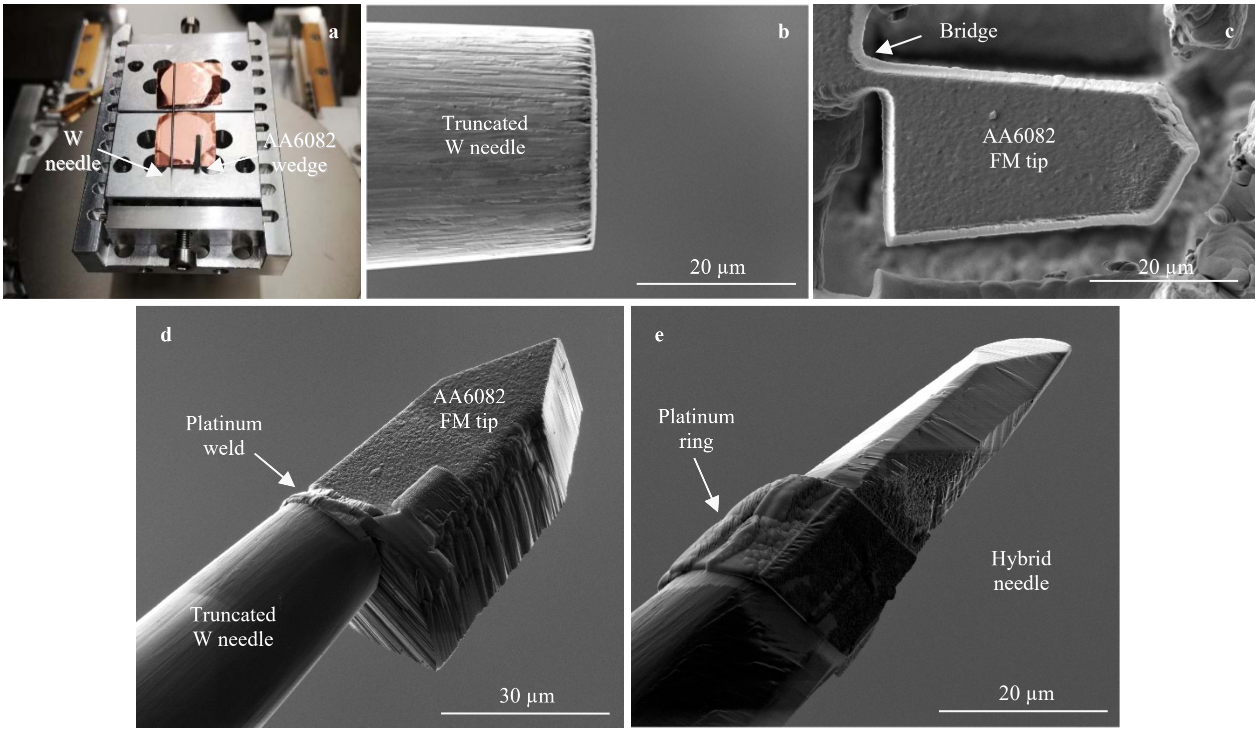

Fig. 3. FIB-assisted needle tip replacement procedure: (a) Picture of the microscope stage showing how the new tungsten (W) needle and the aluminium FM wedge are loaded; (b) W needle after being truncated by ion-milling and ready to be coupled with (c) the FM tip cut out from the AA6082 FM wedge; the tip is being held by a small material bridge; (d) The tip has been transferred on the truncated W needle and secured on that by a temporary platinum weld; (e) Final *hybrid needle* obtained by tip shaping and platinum bonding after multiple needle rotations.

4.1. Preliminary welding setup and failure

The small BM plate was loaded on a simple FIB stub and a oxide-free area was obtained by ion milling of a 0.25 µm deep rectangular pattern. The prepared hybrid needle, secured to the Omniprobe® manipulator, formed an angle of 45° with the BM plate, namely the fixed angle the manipulator forms in the FIB with respect to a horizontal BM sample. The hybrid needle was made approaching the oxide-free surface corner and was pushed along its own axis towards the plate.

The real-time view showed the material from the plate building up in front of the tip, in the pushing direction, blocking the way to further needle moving (Fig.4a). Another attempt was made by pushing the needle along the y axis (parallel to the plate surface). The tip was then observed starting to bend under the pressure load and constrained behind the material barrier that was forming in front of it (Fig.4b). By following pushing, the aluminium tip started bending severely, forming cracks, and suddenly detached from the tungsten base (Fig.4c). The failure occurred at the Al-W interface and the platinum ring resulted to be broken.

The failure reason was identified in a too weak tip geometry that was not able to overcome the excessive friction force generated between the aluminium surfaces: friction was actually expected to make the FM tip deform and be spread onto the BM substrate; Instead, the tip aspect ratio revealed to be too high to bear the substrate resistance and thus instability prevailed on yielding, bringing the tip to failure.

This draws the attention to the necessity of modifying the experimental configuration. Future plans include the same hybrid needle to be pushed perpendicularly inside a hole dig in the BM. This is expected to maximize the shear forces between the materials and to prevent the tip from bending prematurely.

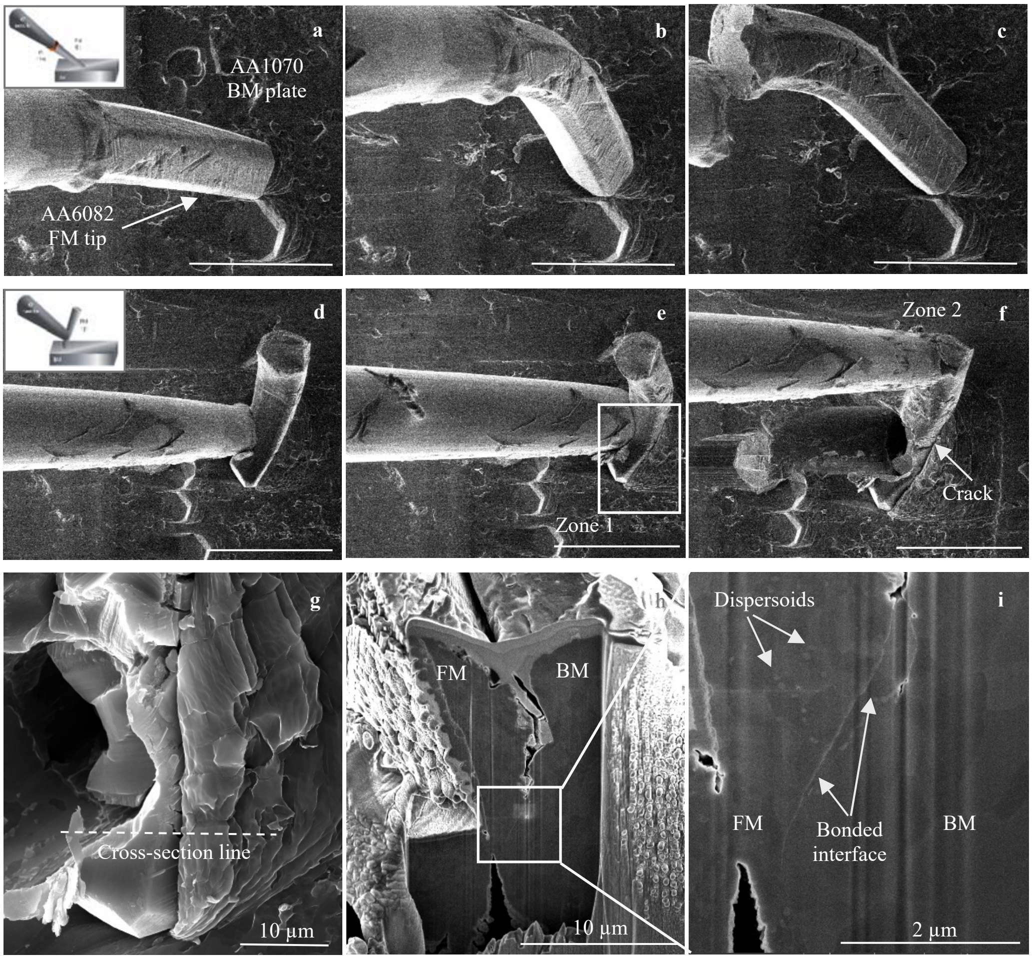

Fig. 4. (a,b,c) SEM pictures of preliminary welding setup sequence: (a) Hybrid needle is being pushed on the BM plate and starts to build up a material barrier in front of its flow; (b) The FM tip bends and some cracks are formed; (c) The FM tip suddenly detach from the tungsten base, by breaking the platinum ring (Scale bar: 30 µm). (d,e,f) SEM pictures of improvised welding setup sequence: (d) After detaching from the BM, the FM tip was held vertical by the material accumulation behind it and the micromanipulator has been employed as a punch on the FM tip; (e) Both BM and FM highly deformed under the pressure load; Possible welding zone identified in the squared area, named as Zone1; (f) By subsequent puching on Zone 2, the FM tip broke from Zone 1, where bond occurred (Scale bar: 50 µm). (g) Magnified picture of welded zone after the experiment; The dotted line is referred to the place where the cross section in (h) was cut from; The squared area in (h) is magnified in (i) where the bonded interface is shown in detail and the differences in microstructure between the coupled materials can be appreciated.

4.2. Final setup and welding

After detaching from the tungsten base needle, the tip remained vertical supported by the material barrier that was previously raised. Therefore, the pushing experiment proceeded by using the truncated tungsten needle as a punch on the FM wire as visible in Fig.4d.

The micromanipulator was moved along its own axis at a speed of 1 µm/s towards the small FM wire piece. The applied pressure resulted to be high enough to highly deform both the workpieces (Fig.4e) and to consequentially to spread the FM onto the BM (Zone 1).

After a first pushing, the needle was retracted and repositioned on a remaining protruding end of the FM piece (Zone 2). Another pushing was carried out on that, with the same parameters, to complete the experiment on all the available material. In this second step, the current stressed part of the FM wire (Zone 2) was observed to crack

(Fig.4f) and detach from the previously deformed part (Zone 1). This means that Zone 1 was held back by a higher force, the bonding one. A preliminary microscale cold pressure welding is considered to be performed successfully.

4.3. Bonded interface analysis

The welding location was identified in the area squared in Fig.4e. Magnified pictures after retracting the punching needle, show the boundary between the bonded materials (Fig.4g). Willing to carry out cross-section analysis on that region, the surface was protected with a deposited platinum layer. Multiple passes of 30 µm deep cleaning cross section patterns were necessary to reveal the entirety of the coupled interface. The alloys microstructure was recognizable at the SEM by operating at 3 kV acceleration voltage and 13 pA current, exploiting Immersion Mode for compensating the low-voltage lower resolution.

In the SEM pictures shown in Fig.4h and Fig.4i, the different alloys in contact are clearly distinguishable: on the left side the AA6082 FM exhibits smaller grains and a higher number of dispersoids, which typically are of iron, manganese and chromium; on the right side the pure aluminium AA1070 BM is bigger in grain size a free from any type of dispersoids or precipitates. Visible porosities still have to be deeper investigated, but they probably belong to the bulk material appearance. The bonded interface appears to be quite limited -certainly due to the poorly designed and improvised pushing setup- but continuous and with a uniform trend. The kissing surfaces look to be compactly joined and this represents a promising result for further experiments. The natural prosecution of the work is to establish a systematical and reproducible procedure that allows to obtain microscale specimens from the joint to assess and optimize its mechanical and electrical properties through proper in-situ testing.

Moreover, EDS analysis were carried out to prove that this is an actual interface between two different alloys. In the silicon and magnesium maps in Fig.5 it is possible to qualitatively appreciate the difference in their content in the two sides: both are slightly denser in the FM side. The spectrum of the selected regions highlights that a higher content of silicon is found in the AA6082 side, the FM region, and in both cases the Si level is consistent with the expected ones (see Tab.1).

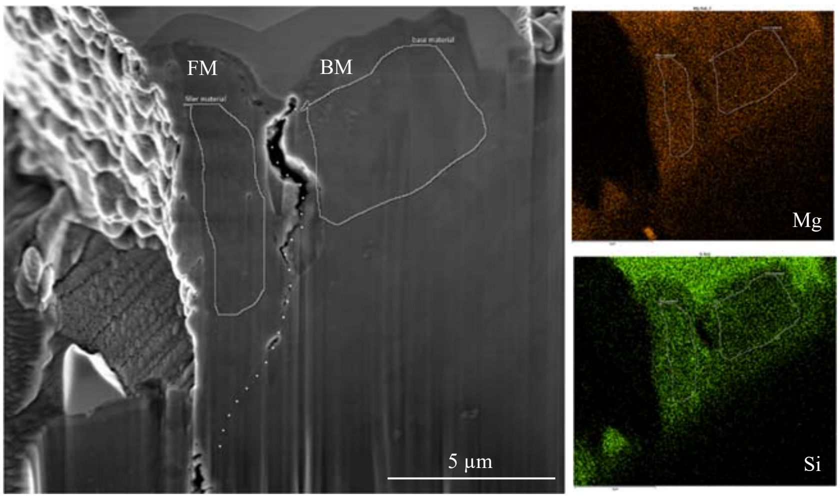

	AA1070 BM		AA6082 FM	
	Nominal	EDS	Nominal	EDS
Si	0.08	0.1	1.11	0.0
Mg	0.01	0.0	0.61	0.6

Fig. 5. EDS analysis on the cross section of the bonded interface. Silicon and magnesium maps show qualitatively that are both denser in the FM side.

Table 1. The silicon and magnesium contents measured by the EDS spectrum was found to be consistent with the nominal ones.

5. Summary

This preliminary work underlined few limitations concerning the designed experimental setup that will represent the starting point for future improvements. Nonetheless, thanks to real-time monitoring of the process, it was possible to adapt the setup in-situ and to prove the feasibility and effectiveness of the joining process at the microscale. The main observations can be sum up as follows:

- It is possible to solid-state weld AA6082 and AA1070 aluminium alloys at the microscale by plastically deforming the two. This phenomenon is a well-established principle happening in the macroscale process of Cold Pressure Welding, which typically results in welded parts stronger than the original materials.
- The microscale joining process was carried out by modifying the micromanipulator needle of a FIB microscope and using it as an actuator on an AA1070 base plate. The tip of the micromanipulator needle has been replaced with an AA6082 tip by means of FIB-assisted micro-fabrication steps. The weld was obtained by pressing the AA6082 tip towards the AA1070 plate.
- The geometrical parameters of the setup are subjected to several degrees of freedom which make the chosen experimental configuration difficult to be controlled and reproduced. Moreover, the designed setup revealed to be weak under different load and friction conditions that made the filler material tip bend and detach from the micromanipulator needle. Improvements are required.
- The setup suggested for the future works is expected to limit bending and to enhance shear stress on the interface between the two materials, to avoid early failure and promote plastic deformation. Repeatably of the process is necessary for further testing of the obtained joints.

References

Aakenes, U. R., Ø. Grong, and T. Austigard. (2014).Application of the Hybrid Metal Extrusion & Bonding (HYB) Method for Joining of AA6082-T6 Base Material, Materials Science Forum, Trans Tech Publications Ltd, 339–44.

Bay, N. (2018).Cold Welding, in *Welding Fundamentals and Processes*, .

Grong, Ø. (2006).Method and Device for Joining of Metal Components, Particularly Light Metal Components,.

Grong, Ø., L. Sandnes, and F. Berto. (2019a).Progress in solid state joining of metals and alloys, Procedia Structural Integrity, 17, 788–98.

---. (2019b).A status report on the hybrid metal extrusion & bonding (HYB) process and its applications, Material Design and Processing Communications, 1, 1–7.

Guo, K. (2008).A Review of Micro/Nano Welding and Its Future Developments, Recent Patents on Nanotechnology, 3, 53–60.

Iordachescu, M., D. Iordachescu, J. Planas, E. Scutelnicu, and J. L. Ocaña. (2009).Material flow and hardening at butt cold welding of aluminium, Journal of Materials Processing Technology, 209, 4255–63.

Lu, Y., J. Y. Huang, C. Wang, S. Sun, and J. Lou. (2010).Cold welding of ultrathin gold nanowires, Nature Nanotechnology, 5, 218–24.

Mayer, J., L. a Giannuzzi, T. Kamino, and J. Michael. (2007).TEM Sample Preparation and FIB-Induced Damage, MRS Bulletin, 32, 400–407.

Misra, A., and C. Daraio. (2009).Sharp carbon-nanotube tips and carbon-nanotube soldering irons, Advanced Materials, 21, 2305–8.

Munroe, P. R. (2009).The application of focused ion beam microscopy in the material sciences, Materials Characterization, 60, 2–13.

Rodriguez-Manzo, J. A., F. Banhart, M. Terrones, H. Terrones, N. Grobert, P. M. Ajayan, B. G. Sumpter, et al. (2009).Heterojunctions between metals and carbon nanotubes as ultimate nanocontacts, Proceedings of the National Academy of Sciences of the United States of America, 106, 4591–95.

Sandnes, L., T. Bergh, Ø. Grong, R. Holmestad, P. E. Vullum, and F. Berto. (2021).Interface microstructure and tensile properties of a third generation aluminium-steel butt weld produced using the Hybrid Metal Extrusion & Bonding (HYB) process, Materials Science and Engineering A, 809.

Sandnes, L., Ø. Grong, J. Torgersen, T. Welo, and F. Berto. (2018).Exploring the hybrid metal extrusion and bonding process for butt welding of Al–Mg–Si alloys, International Journal of Advanced Manufacturing Technology, 98, 1059–65.

Sezen, M. (2016).Focused Ion Beams (FIB) — Novel Methodologies and Recent Applications for Multidisciplinary Sciences, Intech, 32, 137–44.

Sugiyama, M., and G. Sigesato. (2004).A review of focused ion beam technology and its applications in transmission electron microscopy, Journal of Electron Microscopy, 53, 527–36.

Volkert C. A., M. A. M. et al. (2007).Focused Ion Beam Microscopy and Micromachining,.

Wagle, D. V., and G. A. Baker. (2015).Cold welding: A phenomenon for spontaneous self-healing and shape genesis at the nanoscale, Materials Horizons, 2, 157–67.